Journal of Applied Sciences

ISSN 1812-5654

science alert

ANSInet
an open access publisher
http://ansinet.com

Journal of Applied Sciences 8 (8): 1416-1425, 2008
ISSN 1812-5654

Analysis of Photonic Crystal Power Splitters with Different Configurations

A. Ghaffari, F. Monifi, M. Djavid and M.S. Abrishamian
Department of Electrical Engineering, K.N. Toosi University of Technology, Tehran, Iran

Abstract: In this study, power splitters with different lattice configurations are investigated. First a Y-splitter in a square lattice is presented and compared with its counterpart in hexagonal lattice. Then in order to minimize backward reflections and to obtain equal distribution of power we present heterostructure built on hybrid 2-D photonic crystal (PhC) lattice, this structure is a combination of square and hexagonal lattices. Our numeric simulation with finite-difference time-domain (FDTD) technique shows that the heterostructure has better performances. By this structure we achieve an overall throughput efficiency of 94%. Then by applying theoretical approach (Couple Mode theory) transmission properties of T-junctions are optimized and physical mechanism behind them are explained. Also two optimized 90° bend with high transmission efficiency are proposed At last, based on these optimized T-junctions and 90° bends we propose new 1×4 optical power splitter schemes in PhC with high transmission efficiency and equal splitting ratio over a large bandwidth in third communication window.

Key words: Photonic crystal, finite difference time-domain (FDTD), power splitter, unistructure, heterostructure, T-junction

INTRODUCTION

Photonic crystals are artificially engineered materials with periodic arrangement of dielectric constants. They have gained worldwide interest in the past decade. They prohibit propagation of light for frequencies within the Photonic Band Gap (PBG) (Yablonovitch, 1987). There has been an increasing interest in the realization of photonic crystals as optical components and circuits in recent years. Various types of optoelectronic devices such as channel add-drop filters (Ghafari *et al*., 2007; Monifi *et al*., 2007), Mach-Zehnder interferometers (Martinez *et al*., 2005), power splitters (Bayindir *et al*., 2000; Yu *et al*., 2007) and other devices based on PhCs have been investigated. These devices usually have many advantages such as substantial size reduction compared with their conventional counterparts (Joannopoulos *et al*., 1995; Yu *et al*., 2007). Also it is possible to realize low-loss sharp bends in PhC structures. Extensive study on PhC bending waveguides has been done theoretically (Meade *et al*., 1994; Mekis *et al*., 1996) and experimentally (Baba *et al*., 1999).

Optical power splitters are key building blocks in photonic systems. There are different ways to equally split the power of incoming signal into two output ports: for example using directional coupler or Y-junction structures. Photonic crystal optical power splitters based on a Y-junction (Boscolo *et al*., 2002; Lin *et al*., 2002) or T-junction (Fan *et al*., 2001; Sondergaard and Dridi, 2000) have been investigated theoretically or experimentally. Ideally, the splitter should divide an input power equally into output ports without significant reflection or radiation losses and should be compact in size with wide branching angles. To obtain acceptable transmittance, the researchers placed some additional tuning rods in PhCs to optimize the devices.

The main methods for analysis of photonic crystals and especially FDTD method are introduced in the first section. Then transmission characteristics of a unistructure beam splitter built in rectangular and hexagonal lattices is investigated. Then a hybrid Y splitter is proposed, which has higher transmission efficiency in comparison with unistructure splitters. Finally, by using Couple Mode Theory (CMT), transmission properties of a T-shaped junction are optimized. The optimized T-junction and 90° bends are then used in the design of 1×4 power splitters with acceptable properties.

NUMERICAL ANALYSIS

There are various methods for analysis of photonic crystals, including Plane-Wave Expansion (PWE) method, exact Green's function method, transfer matrix method and the FDTD method. The method initially used for

Corresponding Author: Afshin Ghaffari, Department of Electrical Engineering, K.N. Toosi University of Technology, Seyedkhandan, Dr. Shariati Ave, P.O. Box 16315-1355, Tehran, Iran
Tel: +98 21 88462174-7 Fax: +98 21 88462066

theoretical analysis of PhC structures is the plane-wave expansion method, which makes use of the fact that eigenmodes in periodic structures can be expressed as a superposition of a set of plane waves. Although this method can obtain an accurate solution for the dispersion properties of a PhC structure, it has still some limitations. Transmission spectra, field distribution and back reflections cannot be extracted because this method considers only propagating modes. An alternative approach, which has been widely adopted to calculate both transmission spectra and field distribution, is based on numerical solutions of Maxwell equations by use of the FDTD method.

In this study we use both plane-wave and FDTD method in our analysis, the two dimensional FDTD (2D-FDTD) (Taflove, 2005) is used to calculate the spectrum of the power transmission, in our MATLAB code. The computer used in this simulation is P4 3.00 GHz and has 2GB RAM.

For a linear isotropic material in a source-free region, the time-dependent Maxwell's equations can be written in the following form:

$$\frac{\partial H}{\partial t} = -\frac{1}{\mu(r)}\nabla \times E \tag{1}$$

$$\frac{\partial E}{\partial t} = \frac{1}{\varepsilon(r)}\nabla \times H - \frac{\sigma(r)}{\varepsilon(r)}E \tag{2}$$

where, $\varepsilon(r)$, $\mu(r)$and $\sigma(r)$ are the position dependent permitivity, permeability and conductivity of the material, respectively. In the two-dimensional case, the fields can be decoupled into two transversely polarized modes, the E-and H-polarizations. These equations can be discretized in space and time by a so-called Yee-cell technique (Yee, 1966). The following FDTD time stepping formulas are spatial and time discretizations of Eq. 1 and 2 on a discrete two dimensional mesh within the x-y coordinate system for the E-polarization,

$$E_z\Big|_{i,j}^{n+1} = E_z\Big|_{i,j}^{n} + \frac{\Delta t}{\varepsilon_{i,j}}\left[\left(\frac{H_y\Big|_{i+\frac{1}{2},j}^{n+\frac{1}{2}} - H_y\Big|_{i-\frac{1}{2},j}^{n+\frac{1}{2}}}{\Delta x}\right) - \left(\frac{H_x\Big|_{i,j+\frac{1}{2}}^{n+\frac{1}{2}} - H_x\Big|_{i,j-\frac{1}{2}}^{n+\frac{1}{2}}}{\Delta y}\right)\right] \tag{3}$$

$$H_x\Big|_{i,j+\frac{1}{2}}^{n+\frac{1}{2}} = H_x\Big|_{i,j+\frac{1}{2}}^{n-\frac{1}{2}} - \frac{\Delta t}{\mu_0}\left[\frac{E_z\Big|_{i,j+1}^{n} - E_z\Big|_{i,j}^{n}}{\Delta y}\right] \tag{4}$$

$$H_y\Big|_{i+\frac{1}{2},j}^{n+\frac{1}{2}} = H_y\Big|_{i+\frac{1}{2},j}^{n-\frac{1}{2}} - \frac{\Delta t}{\mu_0}\left[\frac{E_z\Big|_{i+1,j}^{n} - E_z\Big|_{i,j}^{n}}{\Delta x}\right] \tag{5}$$

where, the index n denotes the discrete time step, indices i and j denote the discretized grid point in the x-y planes, respectively.

If the following condition is satisfied, FDTD time-stepping formulas are stable numerically:

$$\Delta t \le \frac{1}{c\sqrt{\Delta x^{-2} + \Delta y^{-2}}} \tag{6}$$

where, c is the speed of the light.

The system investigated here is two-dimensional PhC and consists of an array of dielectric rods with refractive index 3.4 (which correspond to GaAs at wavelength of 1.55 μm) in air host. The structure is surrounded by Perfectly Matched Layers (PMLs) (Berenger, 1994) as absorbing boundary conditions to truncate the computational region and to avoid the reflections from the outer boundary. The number of PML layers is set to be 12. Also lattice constant (a) of the structure consists of 21 FDTD grid cells.

The dispersion diagram of the structures is evaluated with a code based on the PWE method. This structure is excited with TM polarization. An adequately broadband Gaussian pulse is launched into input port. Then we placed a detector inside each waveguide channel of the splitter, measuring the time-varying electric and magnetic field.

The electric and magnetic field of the incident and transmitted pulses are stored as a function of time. The output power is calculated at each port by integrating the power over the cells of the output ports as shown in Eq. 7 Then stored data Fourier-transformed and integrated and ratio of transmitted to incident spectra are taken, which results in transmission spectra versus wavelength.

$$P = -\frac{1}{2}\mathrm{Re}\left[\int_{width} E_{y,\omega} H^*_{x,\omega} dx\right] \tag{7}$$

$E_{y,\omega}$ and $H_{x,\omega}$ represent the incident electric and magnetic fields in the frequency domain at the surface of each port.

Y JUNCTION IN DIFFERENT LATTICE CONFIGURATIONS

Here Y splitters in different lattice configurations (Fig. 1) are investigated. A Y-splitter consists of a waveguiding element and a wave splitting element. They are arranged such that each wave splitting element makes a 45° (60°) angle from the main waveguiding element in rectangular (hexagonal) lattice. Our unistructure optical beam splitters consist of silicon rods arranged on a square (hexagonal) lattice in air host.

The lattice constant (a) and the ratio of rod radius to lattice constant (r/a) for rectangular lattice are set to be 543 nm and 0.2, respectively. Also for a Y splitter formed in a hexagonal lattice we set r/a = 0.22 and a = 543 nm.

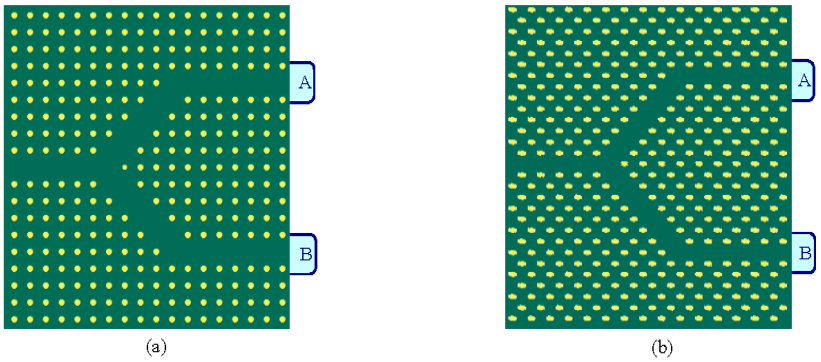

Fig. 1: (a) Y splitter built in a square PhC lattice and (b) Y splitter built in a hexagonal PhC lattice

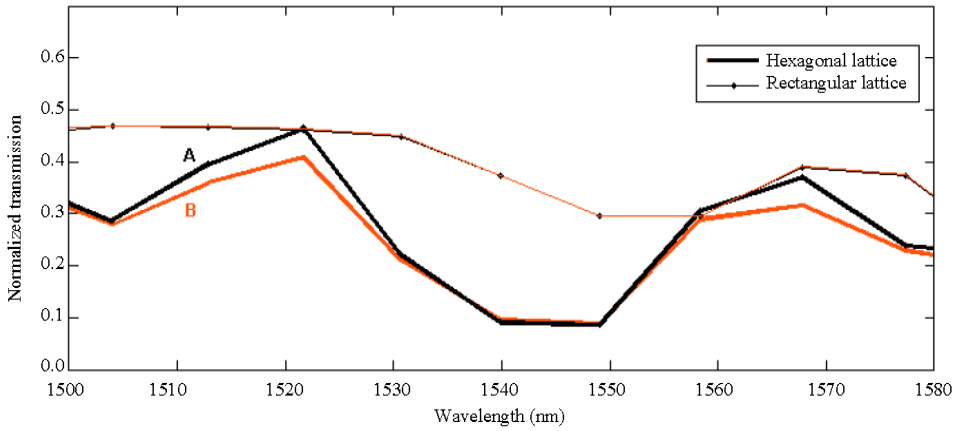

Fig. 2: Transmission spectra for Hexagonal and rectangular lattices for port A (black), port B (red)

This structure has a bandgap for TM-polarized light in the wavelength range $0.28<a/\lambda<0.44$ and $0.27<a/\lambda<0.44$ for rectangular and hexagonal lattice, respectively. Transmission spectra for hexagonal and rectangular lattices are depicted in Fig. 2.

It is seen that Y splitter in hexagonal lattice has poor transmission efficiency in comparison with the one in rectangular lattice although transmission spectra for rectangular lattice is not ideal. So a hybrid structure will be used in our Y splitter to improve its transmission spectra.

HETEROSTRUCTURE Y JUNCTION

A common use for PhCs in integrated optical applications is optical beam splitting or combining which allows for division of an optical beam into multiple signals for density routing. These operations have been limited by the spatial constraints of the single crystalline structure, which in some cases limit their ability to efficiently perform their intended functions.

Limitations such as back reflections and frequency selectivity of certain devices can have a significant impact on the performance and operation of some Photonic-integrated Circuits (PICs). These limitations decrease the performance of an optical device. Therefore in this study we present a design for heterostructure PhC devices that overcomes the limitations mentioned above, in addition to enhancing throughput efficiency and minimizing the back reflections. In order to enhance the throughput efficiency as well as minimizing backward reflections, we use heterostructure (Sharkawy *et al*., 2002) instead of previous single lattice structures. If a PhC is formed from multiple crystalline structures (e.g., square, hexagonal), the newly created structure is no longer a single crystalline structure but a hybrid structure that has the optical characteristics of both structures. The newly formed structure is called a heterostructure PhC. In order to avoid internal mismatches at the interface between the different lattice structures, the structures used in heterostructure must have matched bandgap sizes.

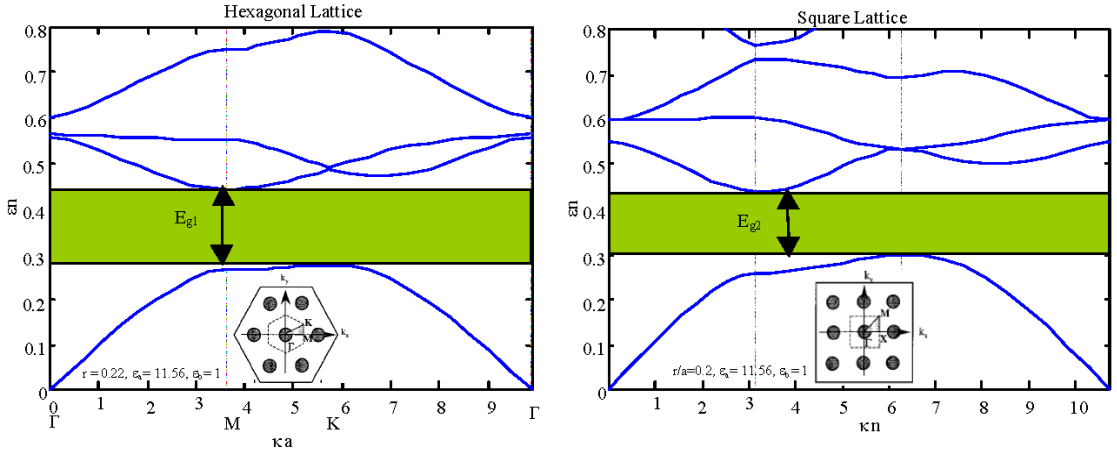

Fig. 3: Band diagram of hexagonal PhC lattice (r/a = 0.22) and square PhC lattice (r/a = 0.2). In Heterostructure both lattices are brought together

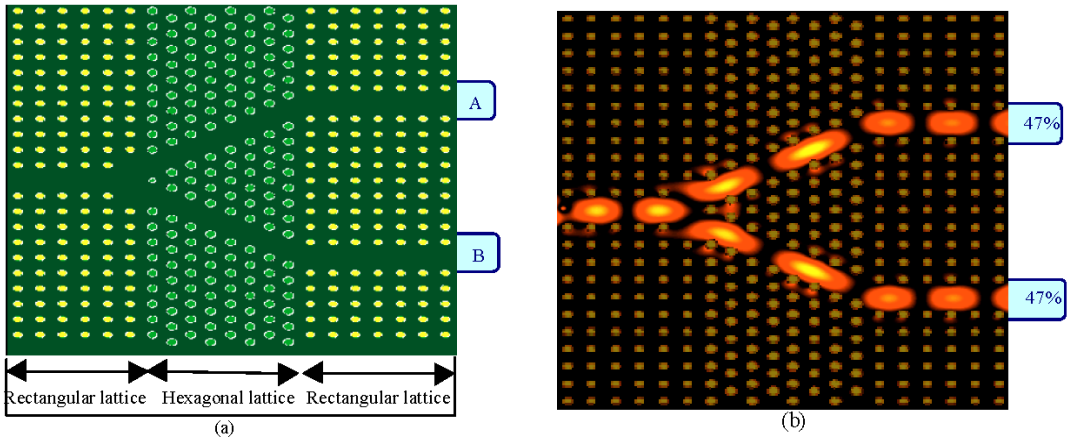

Fig. 4: (a) Y splitter built in a heterostructure PhC (b) The electric field pattern for λ = 1587 nm

When PhCs of different lattice structures are brought together for example, square and hexagonal lattices, we expect discontinuities in their energy bands because each of the structures will have different bandgaps. So we fix the lattice constant in both structures, while varying the radius-to lattice constant ratio r/a for both structures in order to match their bandgaps and minimize $\Delta E_g = E_{g1}-E_{g2}$. We examined both structures using a 2-D plane-wave expansion method for TM polarization; the results are shown in Fig. 3. The optimum r/a values for hexagonal and square lattice structure are 0.22 and 0.2, respectively.

In principle this means that the bandgap obtained from the heterostructure is equivalent to the overlapping of the bandgap of the constituting lattices. Bandgap matching can be useful for applications in which heterostructure PhCs will be used to guide an electromagnetic wave propagating through two different lattices with minimal propagation losses. Heterostructure PhC was used to improve the overall throughput efficiency of a beam splitter by minimizing back reflections mainly caused by mismatches between different sections of the splitter.

The choice of which lattice to be used in each specific part of the heterostructure, is based on the fact that a square lattice is more suited for straight waveguides while for the angular section of the splitter, a hexagonal lattice will be a better candidate. Square lattice is not optimal for guiding a signal through the angular section because this section isn't compatible with a square grid and this will lead to bending losses. We need geometry other than square lattice for the splitting section of the structure that is more suited for that particular section. Hexagonal lattice will provide a lossless transition between the waveguiding and wave-splitting sections.

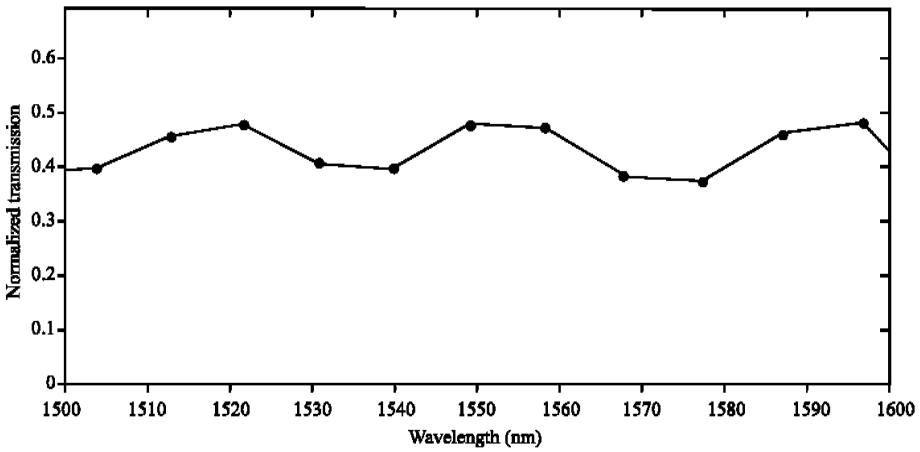

Fig. 5: Heterostructure Y splitter transmission spectra

A Beam splitter formed in a heterostructure PhC is shown in Fig. 4a. The electric field pattern at wavelength 1587 nm is shown in Fig. 4b. Transmission efficiency for each output port is 47% with a total throughput efficiency of about 94%.

The transmission spectra result for this new heterostructure is illustrated in Fig. 5. It is obvious that transmission window corresponding to the unistructure Y splitter has been widened and increased in amplitude in corresponding heterostructure Y splitter.

The loss is mainly because of back reflections at the transition between the waveguiding and the wave-splitting section and bending losses at the corner joints between the angular and the straight waveguide sections. Back reflections at the transition are caused by mismatch between the waveguiding section and the wave-splitting section and hence reduced the overall throughput efficiency of the unistructure beam splitter. Bending losses can be minimized by optimizing the corner joints between the angular waveguide in the hexagonal lattice and the straight waveguide in the square lattice. Geometric parameters, such as the nature of the lattice, the orientation of the line defect in the PhC, the width of the connecting waveguides and the geometry of the branching points have strong effect on energy flow (Sharkawy *et al*., 2002). So in order to minimize backward reflections and to obtain equal distribution of power, branching points of the beam splitter must be designed carefully.

OPTIMIZED T-BRANCH

Here, an optimized T-branch is investigated. In order to reduce the reflection we further investigate the T-branches by referring to (Fan *et al*., 2001). We place some extra rods between the input and output

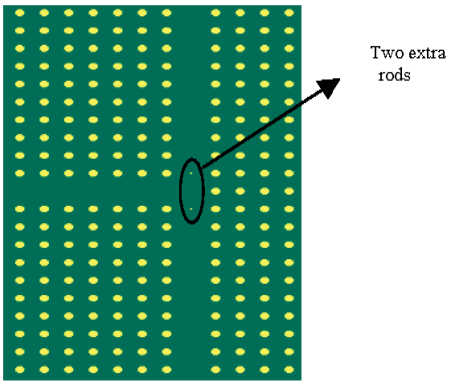

Fig. 6: Optimized T-branch with two extra rods of radius rd = 0.07a

waveguides of the T-branch, as illustrated in Fig. 6.This structure will be investigated numerically. Also in order to analyze it theoretically and explain the physical mechanism of this structure, it is modeled by coupled mode theory.

Theoretical consideration: Now we will use the time-dependent Coupled-Mode Theory (CMT), which was introduced by Haus (1984) and apply it to our cavity splitter. The model focuses on a single-mode cavity with a resonance frequency ω_0 and is characterized by an intrinsic and an external quality factor. The intrinsic quality factor Q_0, also called unloaded quality factor, accounts for the losses inside the cavity (absorption and out-of-plane scattering). It describes the coupling of the cavity modes to the leaky modes above the light line. The external coupling factor Q_e accounts for the energy leakage of the cavity due to the coupling with the waveguide. The value for Q_e is very much dependent on

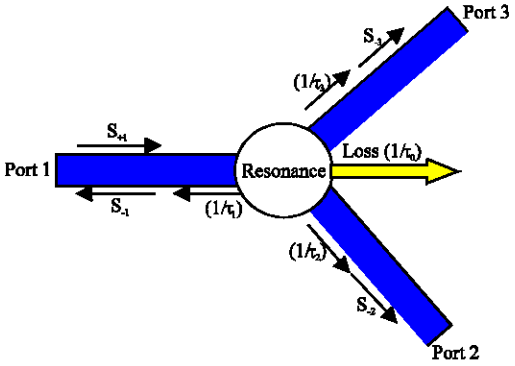

Fig. 7: Sketch of the coupled-mode model of a waveguide branch

the symmetry of the cavity mode with respect to the waveguide modes and is thus very different for each cavity mode (Leunberger, 2004).

According to theoretical modeling based on CMT, in order to obtain a qualitative understanding of waveguide branches in a photonic crystal, we consider the theoretical model shown in Fig. 7.

The temporal CMT is actually based on a temporal differential equation describing the balance between incoming and outgoing field fluxes. In the ideal case with no losses, it is assumed that inside the cavity the field-amplitude oscillates with frequency ω_0 ($a(t) = e^{j\omega 0t}$) and is normalized such that $W = |a|^2$ corresponds to the field energy stored inside the cavity. The cavity may lose energy due to intrinsic losses ($\sim 1/\tau_0$) or due to the coupling to the waveguides ($\sim 1/\tau_i$). Thus in the case where no external wave impinges on the cavity, the amplitude inside the cavity is:

$$a(t) \propto e^{j\omega_0 t}\, e^{-\frac{t}{\tau_0}}\, e^{-\frac{t}{\tau_1}}\, e^{-\frac{t}{\tau_2}}\, e^{-\frac{t}{\tau_3}} \tag{8}$$

The branching region is treated as a cavity that couples to the input and output waveguides. The resonance in the cavity then determines the transport properties of the branch.

The transmission and reflection properties of such a model can be calculated by use of CMT, which relates the incoming and outgoing wave amplitudes S_{+i} and S_{-i} at port i, to the amplitude of the resonant mode a. The power inside the may be increased by an impinging wave with amplitude S_{+i} coupled to the cavity by a coupling constant κ_i and normalized such that $|S_{+i}|^2$ equals the power carried by the incident wave. Taking the time derivative of Eq. 8 and accounting for an incident wave s_{+i} yields:

$$\frac{da(t)}{dt} = j\omega_0 a(t) - \left(\frac{1}{\tau_0} + \frac{1}{\tau_1} + \frac{1}{\tau_2} + \frac{1}{\tau_3}\right) a(t) + \kappa_1 s_{+1} + \kappa_2 s_{+2} + \kappa_3 s_{+3} \tag{9}$$

The coupling coefficient κ_i is depends on the external cavity lifetime τ_i. The relationship between the two quantities $\left(\kappa_i = \sqrt{\frac{2}{\tau_i}}\right)$ is found using the time-reversed symmetry of Maxwell's equations for lossless media ($\tau_0 = \infty$).

Here, $1/\tau_i$ is the amplitude decay rate of the resonance into the *i*th port. Also, for simplicity we have assumed a single-mode cavity. When the electromagnetic wave at a frequency ω is incident upon the system from port 1 and $S_{+2} = S_{+3} = 0$, the reflection coefficient R and the transmission coefficients T_2 and T_3 into the other two ports can be determined as (assuming lossless media ($\tau_0 = \infty$)):

$$R = \left|\frac{S_{-1}}{S_{+1}}\right|^2 = \left|\frac{-j(\omega-\omega_0) + \frac{1}{\tau_1} - \frac{1}{\tau_2} - \frac{1}{\tau_3}}{j(\omega-\omega_0) + \frac{1}{\tau_1} + \frac{1}{\tau_2} + \frac{1}{\tau_3}}\right|^2 \tag{10}$$

$$T_2 = \left|\frac{S_{-2}}{S_{+1}}\right|^2 = \left|\frac{\frac{2}{\sqrt{\tau_1\tau_2}}}{j(\omega-\omega_0) + \frac{1}{\tau_1} + \frac{1}{\tau_2} + \frac{1}{\tau_3}}\right|^2 \tag{11}$$

$$T_3 = \left|\frac{S_{-3}}{S_{+1}}\right|^2 = \left|\frac{\frac{2}{\sqrt{\tau_1\tau_3}}}{j(\omega-\omega_0) + \frac{1}{\tau_1} + \frac{1}{\tau_2} + \frac{1}{\tau_3}}\right|^2 \tag{12}$$

In order to transfer the input power into ports 2 and 3 without reflection at resonance, the decay rates must satisfy following condition:

$$\frac{1}{\tau_1} = \frac{1}{\tau_2} + \frac{1}{\tau_3} \tag{13}$$

The ratio of the power at the two output ports is then

$$\frac{T_2}{T_3} = \frac{\tau_3}{\tau_2} \tag{14}$$

so if $\tau_2 = \tau_3$ the power is equally split between the two ports. Note that, condition (13) is in agreement with the well known theorem of scattering matrix theory according to which it is impossible to match all three ports of a reciprocal lossless three-port system. In a symmetric splitter for example a Y-branch with three-fold symmetry ($\tau_1 = \tau_2 = \tau_3$) operated at resonance frequency, R_{max} and T_{max} that expressed in term of quality factors, become:

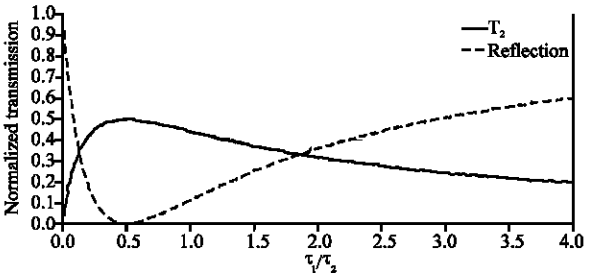

Fig. 8: Results of theoretical model that shown in Fig. 7. Normalized transmission coefficient into port2 and reflection coefficient as a function of the ratio between the decay rates of input and output waveguide

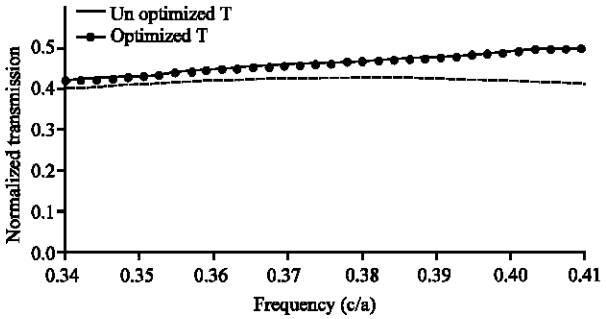

Fig. 9: Transmission spectra of optimized T-branch shown in Fig. 6 and normal T-junction

$$R_{max} = \left| \frac{1+\frac{Q_e}{Q_0}}{3+\frac{Q_e}{Q_0}} \right|^2, \qquad T_{max} = \left| \frac{2}{3+\frac{Q_e}{Q_0}} \right|^2 \tag{15}$$

Therefore for the loss-less case ($Q_e/Q_0 \rightarrow 0$) transmitted intensity into each output port cannot exceed 4/9 of the input intensity. Also the lower limit on the reflection coefficient is 1/9 of the input intensity. In order to overcome the limit of T = 4/9 per arm, we must switch to asymmetric designs where port 1 is slightly different from port 2 and 3.

In Fig. 8, we plot the transmission coefficient T_2 at the resonant frequency as a function of the decay rates τ_1/τ_2, for $\tau_3/\tau_2 = 1$

Numerical simulations: Now based on above mentioned coupled mode theory, in order to reduce the reflection we place some extra rods between the input and output waveguides of the T-branches, as illustrated in Fig. 6. We changed the radii of the extra rods in order to gain highest transmission through the T-junction and we find that the maximum transmission is achieved for an extra-rod radius r_d = 0.07a which agrees with the results of (Fan *et al.*, 2001). Transmission spectra for optimized and conventional (without extra rods) T-junction is depicted in Fig. 9. As it is seen the transmission spectra is significantly improved. We can qualitatively explain the simulation results using the CMT arguments presented above. We approximate the cavity region by a point defect formed by removing one rod from the perfect crystal. The localized state in such a defect should couple to all the input and output waveguides with substantially the same strength. In order to improve the transmission we therefore need to reduce slightly the coupling between the resonance and the output waveguides, to satisfy the rate-matching condition described by Eq. 13. This is achieved by placing extra rods between the input and output waveguides. Although the total structure is no longer symmetric, the constraint (13) is satisfied. By Increasing r_d from zero to r_d = 0.07a (optimal value) transmission improved significantly while further increasing r_d to larger values, results in a deviation from the rate-matching condition and therefore leads to a decrease in transmission.

OPTIMIZING 90° BENDS

Now here, we design two optimized 90° bent waveguides with different bend geometries, which have better transmission properties in comparison with normal bend as shown in Fig. 10a and b. These optimized bends has less reflection due to their optimized geometry.

Bend geometry shown in Fig. 10a provides higher transmission. Also an extra rod with radii rd = 0.7r which placed at the corner of the bend in Fig. 10b reduce the back reflections which results in higher transmission efficiency. Modeling bends by CMT has some limitations because some effects in this model are neglected but these bend geometries can be modeled theoretically by one-dimensional scattering theory as shown by Mekis *et al.* (1996).

In this model for each bend an equivalent effective length is defined. In addition to proposed optimized bends we have recently developed a new 2-D PhC L-shaped bent waveguide based on ring resonators (Javid *et al.*, 2007) which can be used instead of these bends.

In next section these optimized bends will be used in our 1×4 power splitter schemes.

1×4 POWER SPLITTER

Splitters with more than two output ports are needed to be used in photonic networks and 1×4 PhC splitters can become building blocks for compact splitters with more outputs.

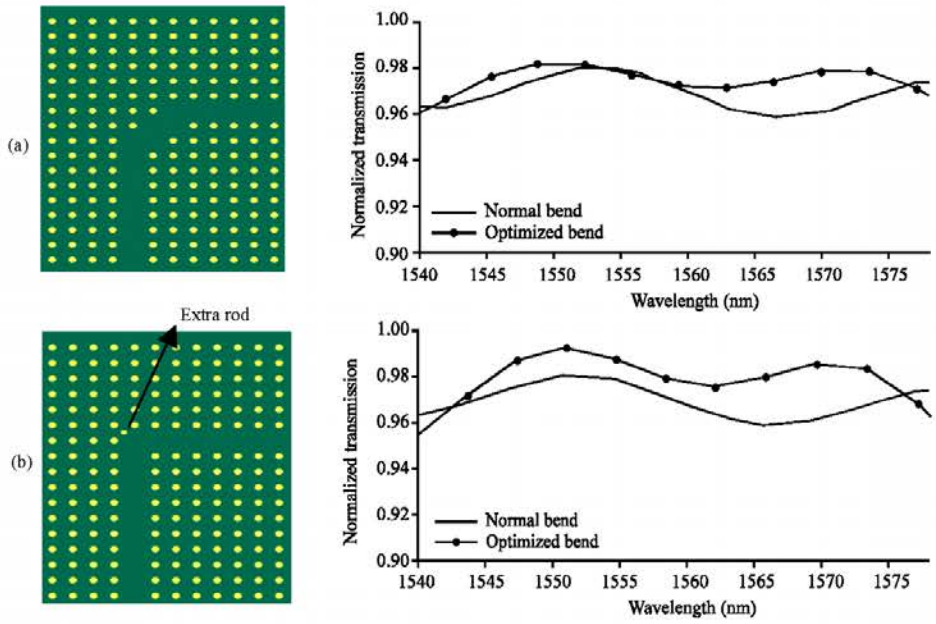

Fig. 10: Normalized transmissions for optimized 90° bend geometries in comparison with normal 90° bend

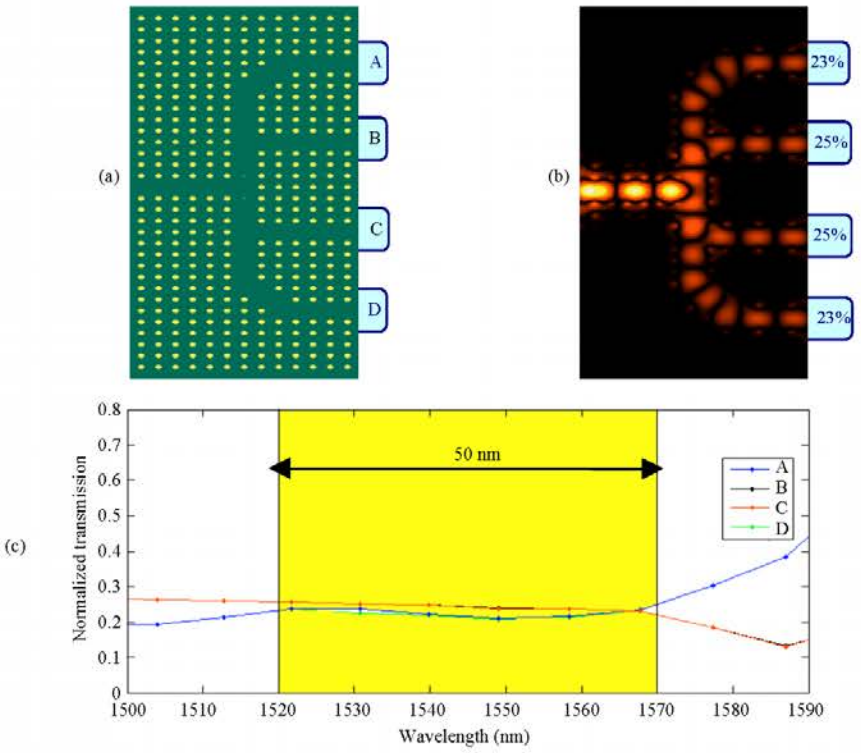

Fig. 11: (a) Schematic of first 1×4 power splitter scheme (b) The electrical field pattern at λ = 1522 nm and (c) Transmission spectra of each port

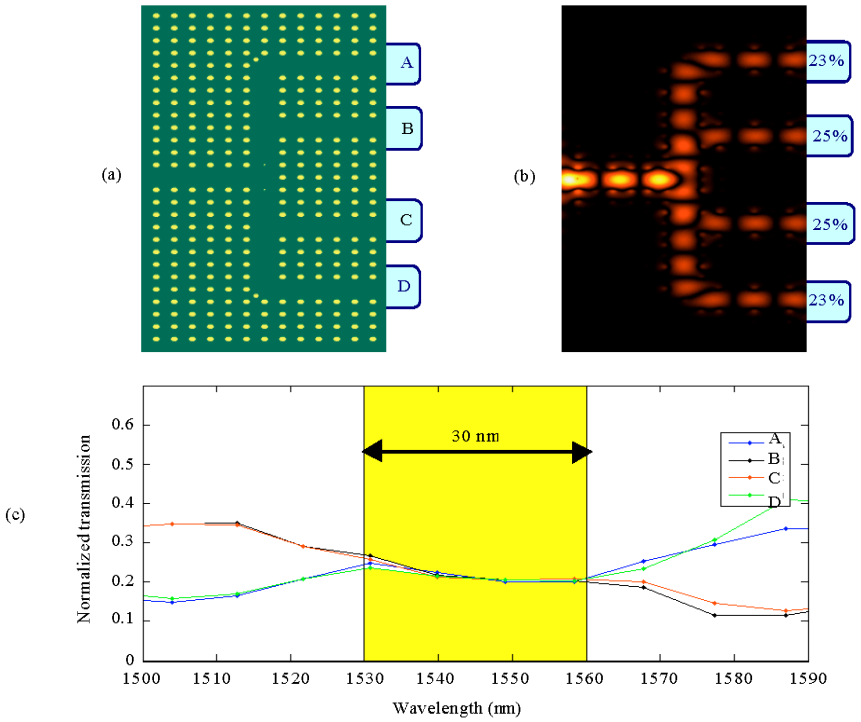

Fig. 12: (a) Schematic of second 1×4 power splitter scheme, (b) The electrical field pattern at λ = 1531 nm and (c) Transmission spectra of each port

Now based on previous optimized 90° bends and T-branches, we propose new 1×4 power splitting schemes and analyze its properties using the FDTD method.

Several cases were tested during an optimization process to maintain 1×4 power splitters with best characteristics. These schemes have high transmission efficiency and equal splitting ratios over a wide bandwidth in the third communication window. The first 1×4 power splitting scheme (Fig. 11a) is based on optimized 90° bend in Fig. 10a and T-branch with two extra rods in Fig. 6. Normalized transmission spectra of each port is depicted in Fig. 11c. It is seen that transmission spectra of port A (B) and D(C) are exact the same. Our acceptable range for this splitter is 50 nm (1520-1570 nm), while there is a slight difference (maximum 3%) between A (B) and C (D).

Another 1×4 power splitter which investigated in this study is depicted in Fig. 12a. This structure consist of optimized bends proposed in Fig. 10b and optimized T-branch. In contrast with first scheme it has narrower acceptable range (30 nm) and lower transmission efficiency, but transmission amplitude of all four ports are exact the same in this range (1530-1560 nm) as shown in Fig. 12c.

CONCLUSION

Several splitter structures were considered in our investigation. They include Y splitters in different lattice configurations like unistructure (rectangular, hexagonal) and heterostructure. Performance of each structure was characterized and compared with each other by transmission coefficients obtained by FDTD code. It has shown that hetrotructure Y splitter has relatively higher transmission efficiency (94% transmission efficiency) in contrast with unistructrures. Then an optimized T-branch and two optimized 90° bends were proposed and compared with their conventional counterparts. In order to explain the physical mechanism behind them we have presented a theoretical analysis (CMT) of T-branch in photonic crystals. Finally based on these optimized bends and T-branches, two 1×4 power splitters were designed. The power flow characteristics of them were also obtained with FDTD simulations which showed that they have high transmission efficiency and equal splitting ratios over a wide bandwidth.

ACKNOWLEDGMENT

This study was supported by Iran Telecommunication Research Center (ITRC).

REFERENCES

Baba, T., N. Fukaya and J. Yonekura, 1999. Observation of light propagation in photonic crystal optical waveguides with bends. Elect. Lett., 35: 654-655.

Bayindir, M., B. Temelkuran and E. Ozbay, 2000. Photonic-crystal-based beam splitters. Applied Phys. Lett., 77: 3902-3904.

Berenger, J.P., 1994. A perfectly matched layer for the absorption of electromagnetic waves. J. Comput. Physics, 114: 185-200.

Boscolo, S., M. Midrio and T.F. Krauss, 2002. Y junctions in photonic crystal channel waveguides: High transmission and impedance matching. Opt. Lett., 27: 1001.

Fan, S., S.G. Johnson, J.D. Joannopoulos, C. Manolatou and H.A. Haus, 2001. Waveguide branches in photonic crystals. J. Optical. Soc. Am. B 18: 162-165.

Ghafari, A., M. Javid, F. Monifi and M.S. Abrishamian, 2007. A numeric analysis of photonic crystal tunable add-drop filters based on ring resonators. IEEE/LEOS Annual Meeting, Florida, USA.

Haus, H.A., 1984. Waves and Field in Optoelectronics. Chap 7. Englewood Cliffs, NJ: Prentice-Hall.

Javid, M., F. Monifi, A. Ghafari and M.S. Abrishamian, 2007. A new broadband L-shaped bend based on photonic crystal ring resonators. PIERS 2008 in Hangzhou Committee. Key: 070807091236 (Posted 11 August (In Press).

Joannopoulos, J.D., R.D. Meade and J.N. Winn, 1995. Photonic Crystals. Princeton U. Press.

Leunberger, D., 2004. Experimental and numerical investigation of two-dimensional photonic crystals for application in integrated optics. Ph.D Thesis, EPFL.

Lin, S.Y., E. Chow, J. Bur, S.G. Johnson and J.D. Joannopoulos, 2002. Low-loss, wide-angle Y splitter at approximately ~1.6- μm wavelengths built with a two-dimensional photonic crystal. Optical. Lett., 27: 1400-1402.

Martinez, A., P. Sanchis and J. Marti, 2005. Mach-Zehnder interferometers in photonic crystals. Opt. Quantum Elect., 37: 77-93.

Meade, R.D., A. Devenyi, J.D. Joannopoulos, O.L. Alerhand, D.A. Smith and K. Kash, 1994. Novel applications of photonic band gap materials: Low-loss bends and high Q cavities. J. Applied Phys., 75: 4753-4755.

Mekis, A., J.C. Chen, I. Kurland, S.H. Fan, P.R. Villeneuve and J.D. Joannopoulos, 1996. High transmission through sharp bends in photonic crystal waveguides. Phys. Rev. Lett., 77: 3787.

Monifi, F., Mehrdad Djavid, Afshin Ghaffari and M.S. Abrishamian, 2007. A new broadband photonic crystal add drop filter. J. Applied Sci. (Accepted).

Sharkawy, A., S. Shi and D.W. Prather, 2002. Heterostructure photonic crystals: Theory and applications. Applied Opt., 41: 7245-7253.

Sondergaard, T. and K.H. Dridi, 2000. Energy Flow in photonic crystal waveguides. Phys. Rev., B 61: 15688-15696.

Taflove, A., 2005. Computational Electrodynamics: The Finite-Difference Time-Domain Method. 3rd Edn. Artech House, Inc.

Yablonovitch, E., 1987. Inhibited spontaneous emission in solid-state physics and electronics. Phys. Rev. Lett., 58: 2059-2062.

Yee, K.S., 1966. Numerical solutions of initial boundary value problems involving Maxwell's equation in isotropic media. IEEE Trans. Antennas Propag, 14: 302.

Yu, T.B., M.H. Wang, X.Q. Jiang, Q.H. Liao and J.Y. Yang, 2007. Ultracompact and wideband power splitter based on triple photonic crystal waveguides directional coupler. J. Opt. A: Pure Applied Opt., 9: 37-42.